

Calculation of spin-Hamiltonian constants for extended defects ($V_{Si}-V_C$)⁰ (Ky5) in silicon carbide polytype 3C-SiC

B.D. Shanina, V.Ya. Bratus'

V. Lashkaryov Institute of Semiconductor Physics, NAS of Ukraine, 41, prospect Nauky, 03680 Kyiv, Ukraine

E-mail: shanina_bela@rambler.ru

Abstract. This work presents theoretical studying the neutral divacancy, *i.e.*, the Ky5 center that is one of the dominant defects in 3C-SiC bulk crystals subjected to relatively high dose of neutron irradiation. Being the paramagnetic center, the extended defect Ky5 shows the value of the zero field splitting (ZFS) in the electron paramagnetic resonance (EPR) signal $D = 443 \cdot 10^{-4} \text{cm}^{-1}$ and $454 \cdot 10^{-4} \text{cm}^{-1}$ in two modifications. To understand the ZFS value, relativistic *ab initio* calculation has been carried out for obtaining the electron structure of 3C-SiC crystal containing the defect Ky5. Using the WIEN program package, the self-consistent values of the electron density ρ and controlling ρ potential V have been found. Based on the obtained values ρ and V , the contributions in ZFS from dipole-dipole and spin-orbit interactions have been found. It has been shown that the main contribution stems from the dipole-dipole interaction. Spin-orbit interaction gives a negligible contribution to ZFS. Due to the relativistic approach, spin-up and spin-down values of the electron density have been obtained, which permits to calculate the hyperfine fields at the nuclei in environment of the divacancy in 3C-SiC.

Keywords: electron paramagnetic resonance, 3C-SiC, electron density, divacancy, zero-field-splitting constant, dipole-dipole and spin-orbit interactions, density functional theory.

doi: <https://doi.org/10.15407/spqeo21.03.225>

PACS 76.30.-v, 73.20.At, 75.70.Tj

Manuscript received 10.07.18; revised version received 04.09.18; accepted for publication 10.10.18; published online 22.10.18.

1. Introduction

An efficiency of SiC-based devices in high-radiation and high-temperature conditions requires considerable attention to irradiation-induced defects and their thermal stability. The possibility of EPR observation for the extended defect (ED) after neutron irradiation is determined by the distribution of electron density in the environment of the extended defects, their electron state energy levels, and ED interaction with crystal field. In the EPR study of the neutron-irradiated cubic SiC samples after thermal annealing within the 200...1100 °C temperature range, the extended paramagnetic defects named Ky5, Ky6, Ky7, and Ky8 were revealed [1, 2]. Based on the previous results, these defects have been attributed to the neutral divacancy ($V_{Si}-V_C$)⁰; negatively charged pair: V_C and carbon anti-site C_{Si} ; negatively charged divacancy; and neutral carbon $\langle 100 \rangle$ split interstitial, respectively.

Provision with commercial wafers of 4H-SiC and 6H-SiC have favored considerable progress in understanding the nature and structure of primary and pair defects in hexagonal SiC modifications in recent

years [2], whereas these aspects are not completely understood in cubic SiC [3-5]. In our previous study, it has been shown that the negatively charged silicon vacancy, the T1 center, and the neutral divacancy, the Ky5 center, are the dominant defects in 3C-SiC bulk crystals neutron-irradiated with a relatively high dose [6]. Some extended defects with spin $S = 1$ demonstrate sufficiently high value of an axial crystalline field $D(\text{Ky5}) = 454 \cdot 10^{-4} \text{cm}^{-1}$; $D(\text{Ky8}) = 606 \cdot 10^{-4} \text{cm}^{-1}$, which requires explanation. D constants were measured also for a set of triplet centers in 6H-SiC [7], all of them have values between 397 and 652 G.

In this work, the results of calculations of the Ky5 defect interaction with crystalline field and constants of super-hyperfine interaction in 3C-SiC have been presented.

It is well known that the constants of crystalline field in spin-Hamiltonian are calculated using the so-called method of equivalent operators developed by Stevens in [8], and described in details in the books [9-11]. All authors call attention on the main limitation of this method that is based on approximation of point charges in the presentation of crystal field. Some

researchers tried to take into account covalent bonds as perturbation to the point charge theory [11, 12], but they remarked the deficiency of this approach. Unlike to the point paramagnetic defects, the extended defects cannot be considered using the theory of point charges. Moreover, in this case there are some other problems: the electron density of the extended defect is not a solution of the equation with the central symmetry potential, its distribution is not known previously, it is not known how many valent electrons from the nearest neighbors of defect take part in formation of the paramagnetic center. Thus, it is necessary to search potential and electron density self-consistently according to the theory by Kohn, Sham, Hohenberg (further KSHS) [13, 14] and program WIEN [15, 16].

It is known that in the case of triplet centers spin-spin, dipole-dipole or spin-orbital interaction give the main contribution to the constant of crystalline field in spin-Hamiltonian [11]. Thus, it is necessary to average these interactions with the found electron density and potential over the defect space.

2. Theoretical basis for calculations of the electron density and crystalline field within the defect range

The calculations of the electronic structure inherent to the defect Ky5 (neutral divacancy $(V_{Si}-V_C)^0$ in the lattice of cubic SiC) were performed using the computer software package WIEN-7k developed by the group of authors [15]. The calculations were based using the density functional theory by KSHS [13, 14].

The full-potential method of the linearized augmented plane waves (FLAPW) was used to solve KSHS equations. The set of the basis wave functions was introduced to two areas of the crystal lattice. The first area I is the non-overlapping spheres of atoms, and the second II is the interatomic space where the electron clouds are overlapped and mixed. The atomic sphere radius R_{at} was chosen in accord with the following two requirements: 1) the sum of R_{at} for two nearest atoms is less or equal the distance between them; 2) the core charge of the atom does not leak out from the atomic sphere. In the first range, the local spin density and the potential are presented as a series of the spherical harmonics Y_{lm} , in the second area they are as a series of plane waves. The solution of KSHS equations is represented as a linear combination of the above basis functions.

$$\rho_{\sigma}^I(r) = \sum_{l,m} c_{lm} Y_{lm}(\mathbf{r}) - \text{inside the atomic sphere,} \quad (1)$$

$$\rho_{\sigma}^{II}(r) = \sum_{\mathbf{k}n} \rho_{\mathbf{k}} \exp(i\mathbf{k}\mathbf{r}) - \text{in the interatomic space.} \quad (2)$$

Here, the vector of the reciprocal lattice is $\mathbf{k} = (2\pi/a) \cdot (\kappa_1, \kappa_2, \kappa_3)$, where $\kappa_1, \kappa_2, \kappa_3$ are the integers.

Coefficients c_{lm} and $\rho_{\mathbf{k}}$ were determined from the condition of values (1) and (2) coincidence at the boundary between the ranges I and II for each plane

wave with \mathbf{k}_n . The total potential that controls the electron density is presented by the same way like (1), (2) in two ranges as two sets:

$$V^I(r) = \sum_{L,M} V_{L,M}(r) \cdot Y_{L,M}(\mathbf{r}) - \text{inside the atomic sphere,} \quad (3)$$

$$V^{II}(r) = \sum_{\mathbf{K}} V_{\mathbf{K}} \exp(i\mathbf{K}\mathbf{r}) - \text{in the interatomic space.} \quad (4)$$

The calculation process for the total energy of the electron system is described in [16]. The exchange-correlation potential was searched in the frame of general gradient approximation (GGA) with parameters of Perdew, Burke, and Ernzerhof [17], where the gradient terms of electron density were included into the exchange-correlation energy and its potential.

The wave functions, charge density, and potential were expanded over the set of spherical harmonics with $L \leq 6$ inside the ‘muffin-tin’ atom radius (R_{at}) equal to 1.9 a.u. and 1.6 a.u. for Si and C atoms, respectively.

At first, calculations of the atomic states for all non-interacting atoms included in the elementary lattice cell were carried out, and the total energy for each isolated atom, $E_{tot,at}(\text{Si}), E_{tot,at}(\text{C})$, was found. All the calculations were performed in the full relativistic approach with the spin polarized electronic states. The self-consistent values ρ and V were achieved with the accuracy $1.0 \cdot 10^{-3}$ a.u.⁻³ for the spin density and 10^{-5} Ry for the energy values.

The wavefunctions obtained at this step form the initial electron density. Using this density, the new Coulomb potential was calculated using the Poisson equation. The potentials were put into KSHS equations, and the new electron density was obtained as the solution of these equations at the first iteration step. After that, the self-consistent iteration process was carried out until the match of solutions for electron density and total energy of system on i -th and $(i-1)$ -th iteration steps was achieved with the required precision.

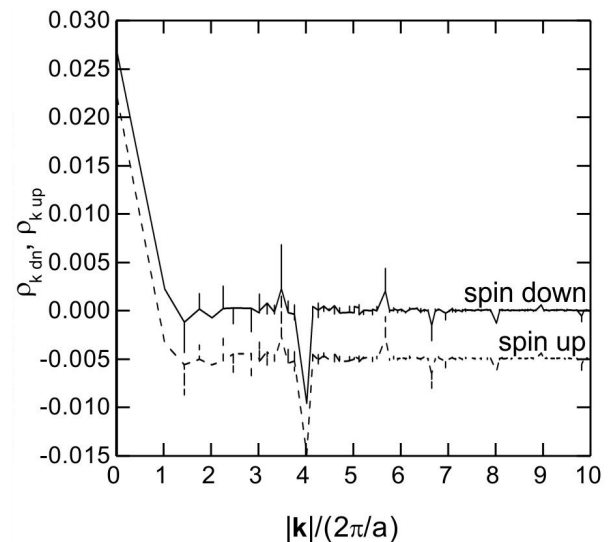


Fig. 1. Decay of $\rho_{\mathbf{k}}$ with increase of the plane wave vector length in ρ -presentation in Eq. (2).

3. Results

Calculations were made for a crystal super-cell as the eight-fold increased primitive cubic cell of 3C-SiC with two vacancies V_{Si} and V_C in the center of the super-cell with the nearest distance between them (position of V_{Si} has the coordinates (0.5; 0.5; 0.5), and carbon vacancy V_C in the site (0.625; 0.625; 0.625). The coordinates are given in relative units to the crystal constant a .

The electron density and the respective potential were obtained as the tables of the expansion coefficients in (1), (1) and (3), (4), respectively. It is impossible to present here the tables because of their large sizes: for example, the sets in (1b), (2b) contain 22957 plane waves.

However, one can see how the coefficients ρ_k in expansion (2) decay with increasing the length of reciprocal lattice vector $|\kappa| = |\mathbf{k}|/(2\pi/a)$. One can see that the largest contribution into $\rho(r)$ is given by small vectors \mathbf{k} with the length $|\mathbf{k}|/(2\pi/a) < 10$.

The projection of electron density with spin down and spin up on the [110] plane is shown in Figs 2 and 3, respectively. The silicon vacancy V_{Si} is located in the center of the plane, while the carbon vacancy is distant from V_{Si} along [111] axis on 1/8 part of the cubic diagonal of the super-cell. As it is seen from Figs 2 and 3, the electron density around the extended defect is formed as the localized state that is the combination of s - and p -like densities. The only symmetry axis of this state is parallel to [111]. The axial crystalline field affecting the paramagnetic defect has the axis of symmetry parallel to the direction [111].

The calculated total density of states (DOS) for the 3C-SiC super-cell with defect $V_{Si}-V_C$ in the center of the cell is presented in Fig. 4. The gap is equal to $E_g = 2.36$ eV. The energy is count down from the Fermi energy (*i.e.*, $E = 0$ in Fig. 4 corresponds to E_F), which is found to be equal to $E_F = 0.614$ Ry in crystal with $V_{Si}-V_C$. It is seen that the localized triplet state with $L = 1$ is in the gap and is split in the crystal field by the singlet 3A_2 and doublet 3E . The Fermi level coincides with the level of deep doublet, because only one defect exists in the cell. The distance of the defect levels from the valence band top is equal to $E_E = 0.920$ eV, $E_A = 0.648$ eV. The defect contributes also the electron states to the bottom of the conduction electron band.

4. Calculation of the spin-Hamiltonian constants for the vacancy pair $V_{Si}-V_C$ in 3C-SiC (paramagnetic center Ky5)

4.1. Hyperfine interaction of the defect electron density with nuclei spin of the surrounding atoms

Full relativistic calculation allows separation of the electron density with spin-up and spin-down, and calculation of the spin density at the nuclei of different atoms in the crystal cell as a difference $\rho_{up}(R_i) - \rho_{dn}(R_i)$, where R_i is a radius-vector of i -th atom. As a result of

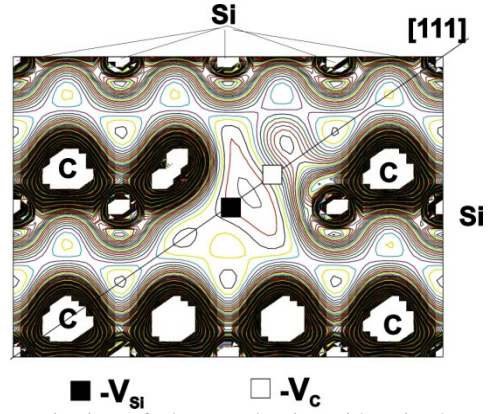


Fig. 2. Projection of electron density with spin down at the plane [110]. Defect Ky5 is located along [111] with V_{Si} in plane center.

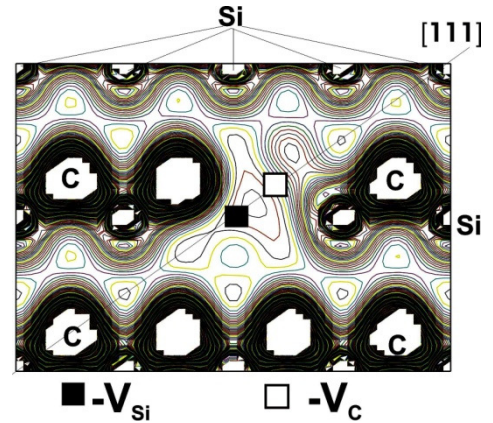


Fig. 3. Projection of electron density with spin up at the plane [110]. Defect Ky5 is located along [111] with V_{Si} in plane center.

computation, convergence of the total energy is achieved with the accuracy 10^{-5} Ry, and the hyperfine field (HFF) at the nuclei of Si and C atoms in the cell is obtained. The contribution of paramagnetic defect is separated by means of subtracting the corresponding HFF in SiC without vacancies. Spin polarization of electron density of core electrons by the spin density of the valence electrons was taken into account.

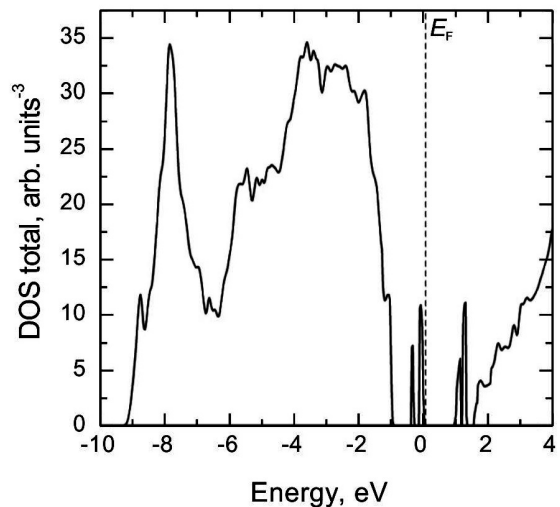


Fig. 4. Total density of states for 8-fold cell of 3C-SiC with the defect $V_{Si}-V_C$.

Hyperfine field HFF at the nuclei was calculated as

$$\begin{aligned} HFF(R_i) &= (4\pi/3) \cdot g\beta \cdot (\rho_{up}(R_i) - \rho_{dn}(R_i)) = \\ &= 5.2431 \cdot 10^5 \cdot \rho_{spin}. \end{aligned} \quad (5)$$

Thereafter the Fermi hyperfine constant was obtained as

$$\begin{aligned} A_s(C) &= HFF(R_{iC}) = 0.388 \cdot 10^{-3} \text{ G}, \\ A_s(\text{Si}) &= HFF(R_{Si,i}) = 0.308 \cdot 10^{-3} \text{ G}. \end{aligned}$$

The constant of dipole-dipole interaction A_p between the spin density of the defect and nuclear spin in the point R_i is found as

$$A_p(R_i) = \frac{2}{3} g\beta g_N \beta_N \left\langle \frac{1}{|\mathbf{R}_i - \mathbf{r}|^3} \right\rangle, \quad (6)$$

where

$$\left\langle \frac{1}{|\mathbf{R}_i - \mathbf{r}|^3} \right\rangle = \iiint_{\Omega_d} \frac{\rho(r)}{|\mathbf{R}_i - \mathbf{r}|^3} r^2 dr \sin \theta d\theta d\varphi. \quad (7)$$

The results are given in Table.

It is seen from Table that the constants of hyperfine interaction for the defect electron spin density with all neighbor atoms are small, except three nearest to V_{Si} carbon atoms C9 that have the Fermi constant $A_s(\text{C9}) = 38.16 \text{ G}$. Unfortunately, the amplitude of the hyperfine component of the EPR spectrum for C9 amounts only 3% of the total EPR signal amplitude, which is rather difficult for observation.

4.2. Crystalline field constants in spin-Hamiltonian of the extended paramagnetic defect

The spin-Hamiltonian term $\mathbf{S} \cdot \mathbf{D} \cdot \mathbf{S}$ is the operator of crystalline field. It includes contributions both from spin-spin dipole-dipole magnetic interaction and from the spin-orbital one. Below, it is fulfilled 'ab initio' calculation of these contributions.

4.2.1. Spin-orbital contribution

In the case of spin-orbital interaction, the operator $\mathbf{S} \cdot \mathbf{D} \cdot \mathbf{S}$ in Hamiltonian is [9]:

$$\mathbf{S} \cdot \mathbf{D} \cdot \mathbf{S} = \lambda^2 \mathbf{S} \Lambda \mathbf{S} \quad (8)$$

with

$$\Lambda_{i,j} = - \sum_n \frac{\langle G | L_i | n \rangle \langle n | L_j | G \rangle}{\epsilon_n - \epsilon_G},$$

λ is the constant of spin-orbital (SO) interaction; L_i – orbital angular moment, $i = 1, 2, 3$; G – ground state of the defect; n is all excited states that are $(2L + 1)$ energy levels split by the crystalline field. Since the paramagnetic defect state is formed by $2p$ -electrons of C-atoms and $3p$ -electrons of Si-atoms from the nearest neighbors of $V_{\text{Si}}-V_{\text{C}}$ defect, their bonding and anti-bonding states exist with different L values, which have different energy levels and most of them are located lower than the valence band edge and upper the conduction band bottom. As it follows from the calculation and picture of the total DOS, only the triplet $|L = 1; M = 0, \pm 1\rangle$ exists in the gap at the Fermi level and a little lower. The initial L -triplet is split by the crystalline field to the singlet with $L_z = 0$ and upper

Table. Hyperfine field (HFF) caused by the defect $V_{\text{Si}}-V_{\text{C}}$ and hyperfine constants at the nuclei of environment.

Atom /(coordinates)	Contribution of Ky5 in HFF, kG	A_s , G	A_p , G	$A_{ }$, G	A_{\perp} , G
$V_{\text{Si}}/(0.5; 0.5; 0.5)$	–	–	–	–	–
$V_{\text{C}}/(0.625; 0.625; 0.625)$	–	–	–	–	–
Si1/(0; 0; 0)	–0.482	–0.14556	0.06549	–0.01458	–0.21105
Si2/(0; 0.25; 0.75)	–0.471	–0.14224	0.20116	0.26008	–0.3434
Si3/(0; 0.75; 0.75)	–0.811	–0.24492	0.25185	0.25877	–0.49677
Si4/(0; 0.25; 0.25)	–1.356	–0.40951	0.16546	–0.0786	–0.57497
Si5/(0.5; 0; 0)	7.69	2.32238	0.11921	2.5608	2.20317
Si6/(0.5; 0.5; 0)	–0.786	–0.23737	0.32807	0.41878	–0.56544
Si7/(0.5; 0.25; 0.75)	–2.59	–0.78218	1.19808	1.61399	–1.98026
Si8/(0.5; 0.75; 0.75)	4.775	1.44205	2.99543	7.4329	–1.55338
Si9/(0.5; 0.25; 0.25)	–10.41	–3.14382	0.68114	–1.78155	–3.82496
C1/(0.125; 0.875; 0.875)	0.389	0.1486	0.25185	0.65229	–0.10325
C2/(0.125; 0.125; 0.125)	0.006	0.00229	0.13919	0.28067	–0.1369
C3/(0.625; 0.875; 0.875)	0.498	0.19024	0.68114	1.55251	–0.4909
C4/(0.125; 0.375; 0.875)	5.962	2.27748	0.32807	2.93363	1.94941
C5/(0.125; 0.125; 0.625)	4.175	1.59485	0.25185	2.09854	1.343
C6/(0.375; 0.625; 0.875)	1.537	0.58713	1.19808	2.9833	–0.61095
C7/(0.125; 0.375; 0.375)	–0.29	–0.11078	0.45235	0.79392	–0.56313
C8/(0.125; 0.625; 0.625)	–0.654	–0.24983	0.68114	1.11244	–0.93097
C9/(0.375; 0.375; 0.625)	99.9	38.1618	2.99543	44.15265	35.16637

doublet with $L_z = \pm 1$. Since the other defect states are distant by a high value $\varepsilon_n - \varepsilon_G$, we can take into account only the doublet state in the sum (6). The distance $\Delta\varepsilon = \varepsilon_2 - \varepsilon_1 = 0.272$ eV.

It would be not correct to calculate (6) using the atomic spin-orbit constants λ_{2p} or λ_{3p} that are determined by the distribution of electron density and potential around the atom. It is necessary to calculate the SO interaction for the defect state with its electron density and crystalline potential. Since the electron density ρ and potential V were obtained self-consistently, 'ab initio' calculation of the λ constant for the defect state is carried out according to the formula [9]

$$\lambda = -\frac{\hbar^2}{2m^2c^2} \cdot \left\langle \frac{1}{r} \cdot \frac{dV}{dr} \right\rangle = -7.4 \cdot 10^{-22} \text{ cm}^2 \left\langle \frac{1}{r} \cdot \frac{dV}{dr} \right\rangle. \quad (9)$$

In Eq. (7), V is the potential expressed in Ry, and r is the electron radius in a.u. = $0.529 \cdot 10^{-8}$ cm. In the case of defect $V_{\text{Si-V}_C}$, calculation is carried out in an inter-atomic space beyond the radius of neighbor atoms around the defect.

$$\left\langle \frac{1}{r} \cdot \frac{dV}{dr} \right\rangle = \int_{\Omega} r^2 dr \sin \theta d\theta d\varphi \rho(r) \frac{dV}{dr} = \sum_{k, k'} \rho_k V_{k'} \int d\Omega \int dr \exp(i\mathbf{k}\mathbf{r}) \frac{d}{dr} (\exp(i\mathbf{k}' \cdot \mathbf{r})). \quad (10)$$

The calculation procedure for (10) consists of the transition to the local coordinate $\mathbf{r}' = \mathbf{r} - \mathbf{R}_0$ with $\mathbf{R}_0 = 0.5625 \cdot (1; 1; 1)$ as the geometrical center of the defect $V_{\text{Si-V}_C}$; expansion of $\exp(i(\mathbf{k}+\mathbf{k}')\mathbf{r})$ over the set of spherical function products [18]; transformation angle functions through the spherical functions $Y_{l,m}(\theta, \varphi)$; using the orthogonality of spherical functions; and integration by θ and φ . Thereafter, one can obtain

$$\left\langle \frac{1}{r} \cdot \frac{dV}{dr} \right\rangle = 2 \sum_{k, k'} \rho_k V_{k'} \cdot \cos \varphi_0 \cdot \frac{\kappa'_1(\kappa_1 + \kappa'_1) - \kappa'_2(\kappa_2 + \kappa'_2) + \kappa'_3(\kappa_3 + \kappa'_3)}{((\kappa'_1 + \kappa_1)^2 + (\kappa'_2 + \kappa_2)^2 + (\kappa'_3 + \kappa_3)^2)^{3/2}} \cdot \int_0^{\mu_{\kappa+\kappa'}} j_1(x) x dx. \quad (11)$$

Here, the values r' , κ , κ' were taken in relative units, i.e., $k = \kappa \cdot 2\pi/a$, $r' = a \cdot r$; γ is the angle between k' and r ; κ_1 , κ_2 , κ_3 are the components of vector \mathbf{k} ;

$$\varphi_0 = 2\pi \cdot 0.5625 \cdot (\kappa_1 + \kappa'_1 + \kappa_2 + \kappa'_2 + \kappa_3 + \kappa'_3). \quad (12)$$

The upper integration limit $\mu_{\kappa+\kappa'} = 2\pi|\kappa + \kappa'| \cdot |r'_{\max}|$, where $r'_{\max} = 0.2$; $j_1(x)$ is the spherical Bessel function in the expansion of exponent by spherical function products. The sum (11) over k, k' was computed and found to be equal to $\left\langle \frac{1}{r} \cdot \frac{dV}{dr} \right\rangle = 2.3 \cdot 10^{-3}$ Ry/a.u.² for

$V_{\text{Si-V}_C}$ defect. Substituting into Eq. (9), we obtain $\lambda = -0.83 \cdot 10^{-6}$ eV, which is by three orders smaller than λ_{2p} of carbon valence electron $\lambda_{2p} = 0.0037$ eV. According to Eq. (8), obtained λ and the value $\Delta\varepsilon = 0.272$ eV give the negligible contribution of spin-orbit interaction (about $1 \cdot 10^{-4}$ G) to D constant.

4.2.2. Calculation of dipole-dipole spin-spin contribution to D constant in the spin-Hamiltonian of the defect $V_{\text{Si-V}_C}$

Contribution of the dipole-dipole spin-spin interaction to the operator of crystalline field is equal to [11]

$$H_{ss} = \frac{3}{4} g^2 \beta^2 \left\langle \frac{r^2 - 3z^2}{r^5} \right\rangle (S_z^2 - (1/3)S(S+1)). \quad (13)$$

Exp. (13) has to be averaged with the calculated electron density in the inter-atomic space of defect Ky5 , i.e.,

$$B = \left\langle \frac{r'^2 - 3z'^2}{r'^5} \right\rangle = \int_{\Omega_d} r'^2 dr' \int \sin \theta d\theta \left(\frac{\rho(r, \theta)}{r'^3} \right) (1 - 3\cos^2 \theta). \quad (14)$$

In what follows, all calculations are carried out in the relative units $r \geq r/a$; $k \geq k/(2\pi/a)$, where a is the size of cubic super-cell. Integration in (13) was made over the volume of defect Ω_d ; $\rho(r, \theta)$ is given in a.u.⁻³. The density $\rho(r, \theta)$ was calculated in the global cubic coordinate system with the origin in the cubic site (0, 0, 0), whereas r' belongs to the integration area. After transition to the local coordinate system with the origin in the centre of distance $V_{\text{Si-V}_C}$, $\mathbf{R}_0 = (0.5625, 0.5625, 0.5625)$ at the axis [1,1,1], radius-vector \mathbf{r} is replaced by $\mathbf{r}' = \mathbf{r} - \mathbf{R}_0$ that is counted from R_0 , and B is integrated over r' in the space of defect. The vectors $\mathbf{k} = (k_1, k_2, k_3)$ are vectors of the reciprocal lattice. Let us expand $\exp(i\mathbf{k}\mathbf{r}')$ over spherical functions $Y_{l,m}(\Omega_1)$, $Y_{l,m}(\Omega_2)$, where $\Omega_{1,2} = (\theta_{1,2}, \varphi_{1,2})$; Ω_2 represents the angles θ_2 and φ_2 , which define the vector \mathbf{k} : $\kappa_1 = \sin\theta_2 \cos\varphi_2$; $\kappa_2 = \sin\theta_2 \sin\varphi_2$; $\kappa_3 = \cos\theta_2$. Replace $(1 - 3\cos^2\theta)$ in (11) with $4(\pi/5)^{1/2} Y_{20}(\theta)$. Normalization of the spherical functions simplifies the expression for B to the following one:

$$B = -4\pi \sum_{k_1, k_2, k_3} R(k_1, k_2, k_3), \quad (15)$$

where

$$\sum_{k_1, k_2, k_3} R(k_1, k_2, k_3) = \sum_k \rho_k \cdot \cos(t_\kappa) \cdot \frac{(3\kappa_3^2 - |\kappa|^2)^{b_1(\kappa)}}{|\kappa|^2} \cdot \int_0^{b_1(\kappa)} \frac{j_2(x)}{x} dx, \quad (16)$$

where $t_\kappa = 2\pi\kappa\mathbf{R}_0 = 3.5343 \cdot (\kappa_1 + \kappa_2 + \kappa_3)$; $r_{\max} = ((3/4\pi)V_{\text{vac}})^{1/3} = 0.195$ for the defect ($V_{\text{Si-V}_C}$); $x = 2\pi\kappa r$; $b_1(\kappa) = 2\pi|r_{\max}| \cdot (\kappa_1^2 + \kappa_2^2 + \kappa_3^2)^{1/2}$.

Now, the spin-spin operator (10) can be written as follows:

$$H_{ss} = D \cdot (S_z^2 - (1/3)S(S+1)),$$

$$D = -9.425 \text{ g}^2 \beta^2 \cdot \sum_{k_1, k_2, k_3} R(k_1, k_2, k_3). \quad (17)$$

It is noteworthy that the electron density is obtained in a.u.⁻³ = 6.76·10²⁴ cm⁻³. Taking it into account and writing D in Gauss, one can obtain

$$D = -118.12 \cdot 10^{-4} \sum_{k_1, k_2, k_3} R(k_1, k_2, k_3). \quad (18)$$

Computation of the sum in (17) over κ gives

$$\sum_{k_1, k_2, k_3} R(k_1, k_2, k_3) = -3.87 \cdot 10^{-4} \text{ for the defect } (V_C - V_{Si})^0,$$

so that the axial crystalline field constant is found to be equal to $D = 489 \cdot 10^{-4} \text{ cm}^{-1}$. This value is close enough to the experimentally found value $D_{exp} = 454 \cdot 10^{-4} \text{ cm}^{-1}$, although it is overestimated.

5. Conclusion

Ab initio calculations in the frame of computational program WIEN gives an opportunity to obtain the space distribution of the self-consistent electron density and potential that controls the electron density. That is sufficient information for calculation of zero field splitting (ZFS) the energy levels of the extended defect. The spin-orbit and dipole-dipole contributions in ZFS of the $V_{Si} - V_C$ defect in 3C-SiC crystal have been calculated in this work. The spin-orbit contribution has been found to be negligible, while the dipole-dipole interaction gives the main contribution to the axial ZFS value.

As it is clear from calculations, in the case when the extended defect includes an atom, contribution of spin-orbital interaction becomes even more significant than that of the dipole-dipole one, since the electron density inside the atomic radius is higher than in the interatomic space.

Acknowledgement

Authors of the paper are grateful for support by National Academy of Sciences of Ukraine (Project № 26/18-H).

References

1. Bratus' V.Ya., Melnik R.S., Okulov S.M., Rodionov V.N., Shanina B.D., Smoliy M.I. A new spin one defect in cubic SiC. *Physica B*. 2009. **404**. P. 4739–4741.
2. Bratus V., Melnyk R., Okulov S., Shanina B., Golub V., Makeeva I. An EPR study of defects in neutron-irradiated cubic SiC crystals. *Mater. Sci. Forum*. 2013. **740–742**. P. 361–364.
3. Isoya J., Umeda T., Mizuochi N., Son N.T., Janzen E., Ohshima T. EPR identification of intrinsic defects in 4H-SiC. *physica status solidi (b)*. 2008. **245**, No 7. P. 1298–1314.
4. Son N.T., Magnusson B., Zolnai Z., Ellison A., Janzen E. Defects in high-purity semi-insulating SiC. *Mater. Sci. Forum*. 2004. **457-460**. P. 437–442.
5. Itoh H., Kawasuso A., Ohshima T., Yoshikawa M., Nashiyama I., Tanigawa S., Misawa S., Okumura H., Yoshida S. Intrinsic defects in cubic silicon carbide. *physica status solidi (a)*. 1997. **162**. P. 173–198.
6. Bratus' V.Ya., Melnyk R.S., Shanina B.D., Okulov S.M. Thermal annealing and evolution of defects in neutron-irradiated cubic SiC. *Semiconductor Physics, Quantum Electronics and Optoelectronics*. 2015. **18**, No 4. P. 403–409.
7. Schollea A., Greulich-Weber S., Raulsc E., Schmidtd W.G., Gerstman U. Fine structure of triplet centers in room temperature irradiated 6H-SiC. *Mater. Sci. Forum*. 2010. **645-648**. P. 403–406.
8. Stevens K. Matrix elements and equivalent operators bound with magnetic properties of rare-earth ions. *Proc. Phys. Soc. A (London)*. 1952. **65**. P. 209.
9. Abragam A., Bleney B. *Electron Paramagnetic Resonance of Transition Ions*. Vol. 2. Clarendon Press, Oxford, 1970.
10. Knox R.S., Gold A. *Symmetry in the Solid State*. Ch.12. New York, Publ. W.A. Benjamin, Inc., 1964.
11. Wertz J.E., Bolton J.R. In book: *Electron Spin Resonance*. Ch. 10. New York, McGraw-Hill Book Co., 1972.
12. Watson R.E., Freeman A.J. Covalency in crystal field theory: KNiF₃. *Phys. Rev. A*. 1964. **134**. P. 1526.
13. Hohenberg P. and Kohn W. Inhomogeneous electron gas. *Phys. Rev*. 1964. **136**. P. B864.
14. Kohn W. and Sham L.J. Self-consistent equations including exchange and correlation effects. *Phys. Rev*. 1965. **140**. P. A1133.
15. Blaha P., Schwarz K., Madsen G.K.H., Kvasnicka D. and Luitz J. *WIEN2k, An Augmented Plane Wave + Local Orbitals Program for Calculating Crystal Properties*. Vienna University of Technology, Vienna, 2001.
16. Weinert M., Wimmer E. and Freeman A.J. Total-energy all-electron density functional method for bulk solids and surfaces. 1982. *Phys. Rev*. **B26**. P. 4571
17. Perdew J.P., Bueke K., Ernzerhof M. Generalised gradient approximation made simple. *Phys. Rev. Lett*. 1996. **77**. P. 3865.
18. Varshalovich D.A., Moscalev A.N., Khersonskii V.K. *Quantum Theory of Angular Momentum* (in Russian). Publ. House "Nauka", Leningrad, 1975 [Published by World Scientific Publishing Co. Pte. Ltd., 1988]; Friedman B., Russek J. Addition theorems for spherical waves. *Quart. of Appl. Math*. 1954. **12**, No 1. P. 13–23.